
TIMEGNN: TEMPORAL DYNAMIC GRAPH LEARNING FOR TIME SERIES FORECASTING

Nancy Xu
KTH Royal Institute of Technology
Stockholm, Sweden
nancyx@kth.se

Chrysoula Kosma
École Polytechnique IPP
Palaiseau, France
kosma@lix.polytechnique.fr

Michalis Vazirgiannis
École Polytechnique IPP
Palaiseau, France
KTH Royal Institute of Technology
Stockholm, Sweden
mvazirg@lix.polytechnique.fr

ABSTRACT

Time series forecasting lies at the core of important real-world applications in many fields of science and engineering. The abundance of large time series datasets that consist of complex patterns and long-term dependencies has led to the development of various neural network architectures. Graph neural network approaches, which jointly learn a graph structure based on the correlation of raw values of multivariate time series while forecasting, have recently seen great success. However, such solutions are often costly to train and difficult to scale. In this paper, we propose TimeGNN, a method that learns dynamic temporal graph representations that can capture the evolution of inter-series patterns along with the correlations of multiple series. TimeGNN achieves inference times 4 to 80 times faster than other state-of-the-art graph-based methods while achieving comparable forecasting performance.

Keywords Time Series Forecasting · Graph Structure Learning · GNNs

1 Introduction

From financial investment and market analysis [1] to traffic [2], electricity management, healthcare [3], and climate science, accurately predicting the future real values of series based on available historical records forms a coveted task over time in various scientific and industrial fields. There are a wide variety of methods employed for time series forecasting, ranging from statistical [4] to recent deep learning approaches [5]. However, there are several major challenges present. Real-world time series data are often subject to noisy and irregular observations, missing values, repeated patterns of variable periodicities and very long-term dependencies.

While the time series are supposed to represent continuous phenomena, the data is usually collected using sensors. Thus, observations are determined by a sampling rate with potential information loss. On the other hand, standard sequential neural networks, such as recurrent (RNNs) [6] and convolutional networks (CNNs) [7], are discrete and assume regular spacing between observations. Several continuous analogues of such architectures that implicitly handle the time information have been proposed to address irregularly sampled missing data [8, 9].

The variable periodicities and long-term dependencies present in the data make models prone to shape and temporal distortions, overfitting and poor local minima while training with standard loss functions (e. g., MSE). Variants of DTW and MSE have been proposed to mitigate these phenomena and can increase the forecasting quality of deep neural networks [10, 11].

A novel perspective for boosting the robustness of neural networks for complex time series is to extract representative embeddings for patterns after transforming them to another representation domain, such as the spectral one. Spectral approaches have seen much use in the text domain. Graph-based text mining (i. e., Graph-of-Words) [12] can be used for capturing the relationships between the terms and building document-level representations.

It is natural, then, that such approaches might be suitable for more general sequence modeling. Capitalizing on the recent success of graph neural networks (GNNs) on graph structured data, a new family of algorithms jointly learns a correlation graph between interrelated time series while simultaneously performing forecasting [13, 14, 15]. The nodes in the learnable graph structure represent each individual time series and the links between them express their temporal similarities. However, since such methods rely on series-to-series correlations, they do not explicitly represent the inter-series temporal dynamics evolution.

Some preliminary studies have proposed simple computational methods for mapping time series to temporal graphs where each node corresponds to a time step, such as the visibility graph [16] and the recurrence network [17]. In this paper, we propose a novel neural network, *TimeGNN*, that extends these previous approaches by jointly learning dynamic temporal graphs for time series forecasting on raw data. TimeGNN (i) extracts temporal embeddings from sliding windows of the input series using dilated convolutions of different receptive sizes, (ii) constructs a learnable graph structure, which is forward and directed, based on the similarity of the embedding vectors in each window in a differentiable way, (iii) applies standard GNN architectures to learn embeddings for each node and produces forecasts based on the representation vector of the last time step.

We evaluate the proposed architecture on various real-world datasets and compare it against several deep learning benchmarks, including graph-based approaches. Our results indicate that TimeGNN is significantly less costly in both inference and training while achieving comparable forecasting performance.

2 Related Work

Time series forecasting models. Time series forecasting has been a long-studied challenge in several application domains. In terms of statistical methods, linear models including the autoregressive integrated moving average (ARIMA) [4] and its multivariate extension, the vector autoregressive model (VAR) [18] constitute the most dominant approaches. The need for capturing non-linear patterns and overcoming the strong assumptions for statistical methods, e. g., the stationarity assumption, has led to the application of deep neural networks, initially introduced in sequential modeling, to the time series forecasting setting. Those models include recurrent neural networks (RNNs) [6] and their improved variants for alleviating the vanishing gradient problem, namely the LSTM [19] and the GRU [20]. An alternative method for extracting long-term dependencies via large receptive fields can be achieved by leveraging stacked dilated convolutions, as proposed along with the Temporal Convolution Network (TCN) [21]. Bridging CNNs and LSTMs to capture both short-term local dependency patterns among variables and long-term patterns, the Long- and Short-term Time-series network (LSTNet) [22] has been proposed. For univariate point forecasting, the recently proposed N-BEATS model [23] introduces a deep neural architecture based on a deep stack of fully-connected layers with basis expansion. Attention-based approaches have also been employed for time-series forecasting, including Transformer [24] and Informer [25]. Finally, for efficient long-term modeling, the most recent Autoformer architecture [26] introduces an auto-correlation mechanism in place of self-attention, which extracts and aggregates similar sub-series based on the series periodicity.

Graph neural networks. Over the past few years, graph neural networks (GNNs) have been applied with great success to machine learning problems on graphs in various fields, including chemistry for drug screening [27] and biology for predicting the functions of proteins modeled as graphs [28]. The field of GNNs has been largely dominated by the so-called message passing neural networks (MPNNs) [29], where each node updates its feature vector by aggregating the feature vectors of its neighbors. In the case of time series data on arbitrary known graphs, e. g., in traffic forecasting, several architectures that combine sequential models with GNNs have been proposed [2, 30, 31, 32].

Joint graph structure learning and forecasting. However, since spatial-temporal forecasting requires an a priori topology which does not apply in the case of most real-world time series datasets, graph structure learning has arisen as a viable solution. Recent models perform joint graph learning and forecasting for multivariate time series data using GNNs, intending to capture temporal patterns and exploit the interdependency among time series while predicting the series' future values. The most dominant algorithms include NRI [33], MTGNN [13] and GTS [15], in which the graph nodes represent the individual time series and their edges represent their temporal evolution. MTGNN obtains the graph adjacency from the as a degree- k structure from the pairwise scores of embeddings of each series in the multivariate collection, which might pose challenges to end-to-end learning. On the other hand, NRI and GTS employ the Gumbel softmax trick [34] to sample from the edge probabilities a discrete adjacency matrix in a differentiable way. Both models compute fixed-size representations of each node based on the time series, with the former dynamically producing the representations per individual window and the latter extracting global representations from the whole training series. MTGNN combines temporal convolution with graph convolution layers, and GTS uses a Diffusion Convolutional Recurrent Neural Network (DCRNN) [2], where the hidden representations of nodes are diffused using graph convolutions at each step.

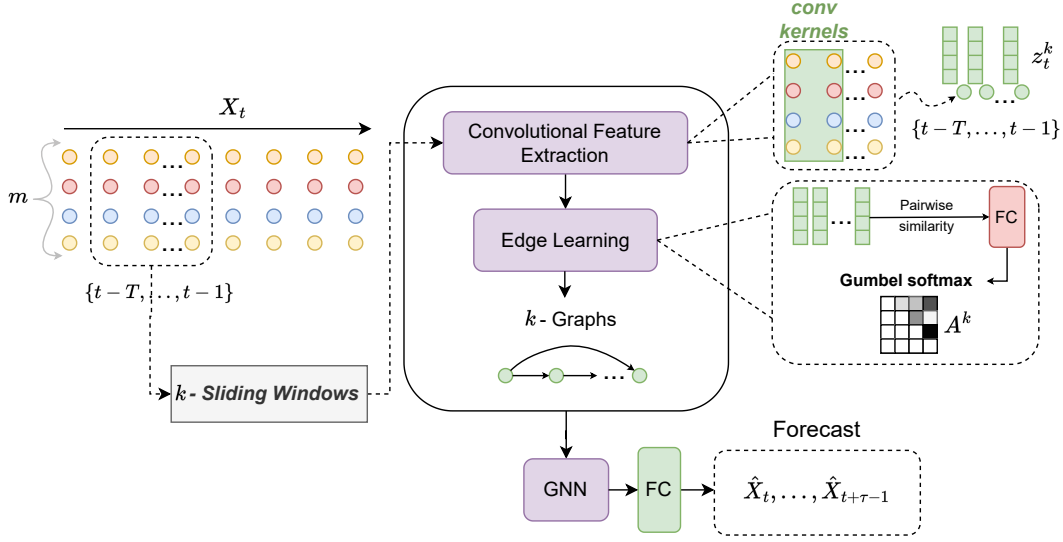


Figure 1: The proposed TimeGNN framework for graph learning from raw time series and forecasting based on embeddings learned on the parameterized graph structures.

3 Method

Let $\{X_{it}\} \in \mathbb{R}^{m \times L}$ be a multivariate time series. Each time series consists of m channels and has a length equal to L which corresponds to the observation times $\{t_1, t_2, \dots, t_L\}$. Then, $\mathbf{X}_t \in \mathbb{R}^m$ represents the observed values at time step t . Let also \mathcal{G} denote the set of temporal dynamic graph structures that we want to infer.

Given the observed values of T previous time steps of the time series, i. e., $\mathbf{X}_{t-T}, \dots, \mathbf{X}_{t-1}$, the goal is to forecast the next τ time steps ($\tau = 1$ for 1-step forecasting), i. e., $\hat{\mathbf{X}}_t, \hat{\mathbf{X}}_{t+1}, \dots, \hat{\mathbf{X}}_{t+\tau-1}$. These values can be obtained by the forecasting model \mathcal{F} with parameters Φ and the graphs \mathcal{G} as follows:

$$\hat{\mathbf{X}}_t, \hat{\mathbf{X}}_{t+1}, \dots, \hat{\mathbf{X}}_{t+\tau-1} = \mathcal{F}(\mathbf{X}_{t-T}, \dots, \mathbf{X}_{t-1}; \mathcal{G}; \Phi) \quad (1)$$

3.1 Time Series Feature Extraction

Unlike previous methods which extract one feature vector per variable in the multivariate input, our method extracts one feature vector per time step in each window k of length T . More specifically, temporal sub-patterns are learned using stacked dilated convolutions, similar to the main blocks of the inception architecture [35].

Given the sliding windows $\mathbf{S} = \{\mathbf{X}_{t-T+k-K}, \dots, \mathbf{X}_{t+k-K-1}\}_{k=1}^K$, we perform the following convolutional operations to extract three feature maps $\mathbf{f}_0^k, \mathbf{f}_1^k, \mathbf{f}_2^k$, per window \mathbf{S}^k . Let $\mathbf{f}_i^k \in \mathbb{R}^{T \times d}$ for hidden dimension d of the convolutional kernels, such that:

$$\begin{aligned} \mathbf{f}_0^k &= \mathbf{S}^k * \mathbf{C}_0^{1,1} + \mathbf{b}_{01} \\ \mathbf{f}_1^k &= (\mathbf{S}^k * \mathbf{C}_1^{1,1} + \mathbf{b}_{11}) * \mathbf{C}_2^{3,3} + \mathbf{b}_{23} \\ \mathbf{f}_2^k &= (\mathbf{S}^k * \mathbf{C}_2^{1,1} + \mathbf{b}_{21}) * \mathbf{C}_2^{5,5} + \mathbf{b}_{25} \end{aligned} \quad (2)$$

where $*$ the convolutional operator, $\mathbf{C}_0^{1,1}, \mathbf{C}_1^{1,1}, \mathbf{C}_2^{1,1}$ convolutional kernels of size 1 and dilation rate 1, $\mathbf{C}_2^{3,3}$ a convolutional kernel of size 3 and dilation rate 3, $\mathbf{C}_2^{5,5}$ a convolutional kernel of size 5 and dilation rate 5, and $\mathbf{b}_{01}, \mathbf{b}_{11}, \mathbf{b}_{21}, \mathbf{b}_{23}, \mathbf{b}_{25}$ the corresponding bias terms.

The final representations per window k are obtained using a fully connected layer on the concatenated features $\mathbf{f}_0^k, \mathbf{f}_1^k, \mathbf{f}_2^k$, i. e., $\mathbf{z}^k = \text{FC}(\mathbf{f}_0^k \parallel \mathbf{f}_1^k \parallel \mathbf{f}_2^k)$, such that $\mathbf{z}^k \in \mathbb{R}^{T \times d}$. In the next sections, we refer to each time step of the hidden representation of the feature extraction module in each window k as $\mathbf{z}_i^k, \forall i \in \{1, \dots, T\}$.

3.2 Graph Structure Learning

The set $\mathcal{G} = \{\mathcal{G}^k\}, k \in \mathbb{N}^*$ describes the collection of graph structures that are parameterized for all individual sliding window of length T of the series, where K defines the total number of windows. The goal of the graph learning module is to learn each adjacency matrix $\mathbf{A}^k \in \{0, 1\}^{T \times T}$ for a temporal window of observations \mathbf{S}^k . Following the works of [33, 15], we use the Gumbel softmax trick to sample a discrete adjacency matrix as described below.

Let \mathbf{A}^k be a random variable of the matrix Bernoulli distribution parameterized by $\theta^k \in [0, 1]^{T \times T}$, so that $A_{ij}^k \sim \text{Ber}(\theta_{ij}^k)$ is independent for pairs (i, j) . By applying the Gumbel reparameterization trick [34] for enabling differentiability in sampling, we can obtain the following:

$$\begin{aligned} A_{ij}^k &= \sigma((\log(\theta_{ij}^k/(1 - \theta_{ij}^k)) + (\mathbf{g}_{i,j}^1 - \mathbf{g}_{i,j}^2))/s), \\ \mathbf{g}_{i,j}^1, \mathbf{g}_{i,j}^2 &\sim \text{Gumbel}(0, 1) \forall i, j \end{aligned} \quad (3)$$

where $\mathbf{g}_{i,j}^1, \mathbf{g}_{i,j}^2$ vectors of i.i.d samples drawn from Gumbel distribution, σ the sigmoid activation and s a parameter that controls the smoothness of samples, so that the distribution converges to categorical values when $s \rightarrow 0$. The link predictor is applied on each pair of extracted features $(\mathbf{z}_i^k, \mathbf{z}_j^k)$ of window k and maps their similarity to a $\theta_{ij}^k \in [0, 1]$ by applying fully connected layers and a sigmoid activation:

$$\theta_{ij}^k = \sigma\left(\text{FC}(\text{FC}(\mathbf{z}_i^k \parallel \mathbf{z}_j^k))\right) \quad (4)$$

In order to obtain directed and forward (i. e., no look-back in previous time steps in the history) graph structures \mathcal{G} we only learn the upper triangular part of the adjacency matrices.

3.3 Graph Neural Network for Forecasting

Once the collection \mathcal{G} of learnable graph structures per sliding window k are sampled, standard GNN architectures can be applied for capturing the node-to-node relations, i. e., the temporal graph dynamics. GraphSAGE [36] was chosen as the basic building GNN block of the node embedding learning architecture. GraphSAGE can effectively generalize across different graphs with the same attributes, which is fitting for this task. GraphSAGE is an inductive framework that exploits node feature information and generates node embeddings (i. e., \mathbf{h}_u for node u) via a learnable function, by sampling and aggregating features from a node’s local neighborhood (i. e., $\mathcal{N}(u)$).

Let $(\mathcal{V}^k, \mathcal{E}^k)$ correspond to the set of nodes and edges of the learnable graph structure for each \mathcal{G}^k . The node embedding update process for each $p \in \{1, \dots, P\}$ aggregation steps, employs the mean-based aggregator, namely convolutional, by calculating the element-wise mean of the vectors in $\{\mathbf{h}_u^{p-1}, \forall u \in \mathcal{N}(u)\}$, such that:

$$\mathbf{h}_u^p \leftarrow \sigma(\mathbf{W} \cdot \text{MEAN}(\{\mathbf{h}_u^{p-1}\} \cup \{\mathbf{h}_u^{p-1} \forall u \in \mathcal{N}(u)\})) \quad (5)$$

where \mathbf{W} trainable weights. The final normalized (i. e., $\tilde{\mathbf{h}}_u^p$) representation of the last node (i. e., time step) in each forward and directed graph denoted as $\mathbf{z}_{u_T} = \tilde{\mathbf{h}}_{u_T}^p$ is passed to the output module. The output module consists of two fully connected layers which reduce the vector into the final output dimension, so as to correspond to the forecasts $\hat{\mathbf{X}}_t, \hat{\mathbf{X}}_{t+1}, \dots, \hat{\mathbf{X}}_{t+\tau-1}$. Figure 1 demonstrates the several components of the proposed TimeGNN architecture, including feature extraction, graph learning, GNN and output modules for forecasting.

3.4 Training & Inference

To train the parameters of Equation 1 for the time series point forecasting task, we use the mean absolute loss. Let $\hat{\mathbf{X}}^i, i \in \{1, \dots, K\}$ denote the predicted vector values for K samples then the MAE loss is defined as:

$$\text{MAE} = \frac{1}{K} \sum_{i=1}^K \|\hat{\mathbf{X}}^i - \mathbf{X}^i\|$$

The optimized weights for the feature extraction, graph structure learning and GNN and output modules are selected based on the minimum loss during training, which is evaluated as described in the experimental setup (section 4.3)

4 Experimental Evaluation

We next describe the experimental setup, including the datasets and baselines we use for comparisons. We also demonstrate and analyze the results obtained by employing the proposed TimeGNN architecture and the baseline models.

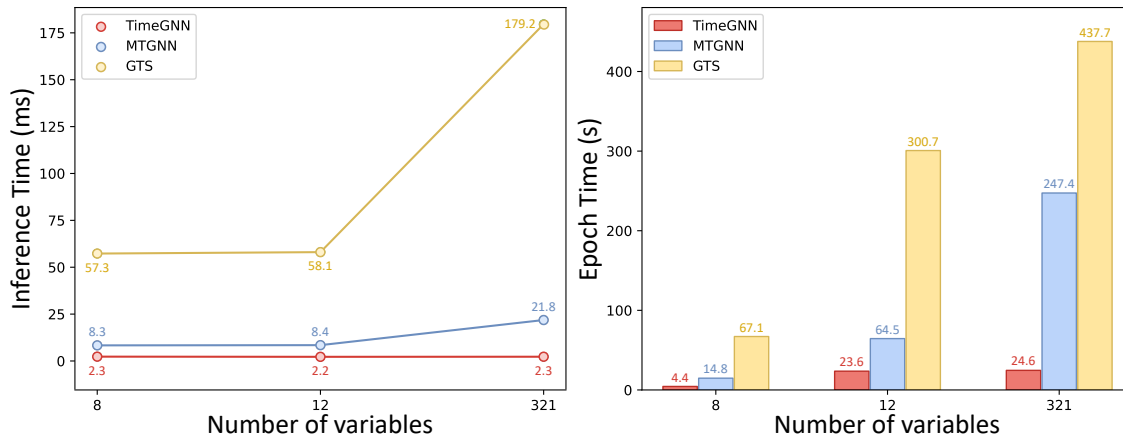


Figure 2: Computation cost of varying number of variables for graph-based models.

4.1 Datasets

This work was evaluated on the following multivariate time series datasets:

Exchange-Rate which consists of the daily exchange rates of 8 countries from 1990 to 2016, following the preprocessing of [22].

Weather that contains hourly observations of 12 climatological features over a period of four years¹, preprocessed as in [25].

Electricity-Load which is based on the UCI Electricity Consuming Load dataset² that records the electricity consumption of 370 Portuguese clients from 2011 to 2014. As in [25], the recordings are binned into hourly intervals over the period of 2012 to 2014 and clients reduced to 321 due to missing information.

4.2 Baselines

We consider five baseline models for comparisons for time series forecasting. We chose two graph methods, MTGNN[13] and GTS[15], and three non-graph methods, LSTNet[22], LSTM[19], and TCN[21]. For LSTM and TCN, the size of the hidden dimension and number of layers follow TimeGNN. In this paper they are fixed to three layers with hidden dimensions of 32, 64, and 128 for the Exchange-Rate, Weather, and Electricity datasets respectively. In the case of MTGNN, GTS, and LSTNet, parameters were kept as close as possible to the ones mentioned in their experimental setups including training loss and optimizers.

4.3 Experimental Setup

Each model is trained for two runs for 50 epochs and the average mean squared error (MSE), mean absolute error (MAE), and R^2 score on the test set are recorded. The model chosen for evaluation is either the model that performs the best on the validation set during training or the final model after 50 epochs, whichever scores better.

The same dataloader is used for all models where the train, validation, and test splits are 0.7, 0.1, and 0.2 respectively. The data is split first and each split is scaled using the standard scalar. The dataloader uses windows of length 96 and batch size 16. The forecasting horizons tested are 1, 3, 6, and 9 time steps into the future, where the exact value of the time step is dependent on the dataset (eg, 3 time steps would correspond to 3 hours into the future for the weather dataset and 3 days into the future for the exchange dataset). In this paper, we use single-step forecasting for ease of comparison with other baseline methods. For training, we use the Adam optimizer with a learning rate of 0.001.

Models are trained on the Alvis cluster at National Academic Infrastructure for Supercomputing in Sweden (NAISS). Experiments for the Weather and Exchange datasets were conducted on an NVIDIA T4 and Electricity on an NVIDIA A40.

¹<https://www.ncei.noaa.gov/data/local-climatological-data/>

²<https://archive.ics.uci.edu/ml/datasets/ElectricityLoadDiagrams20112014>

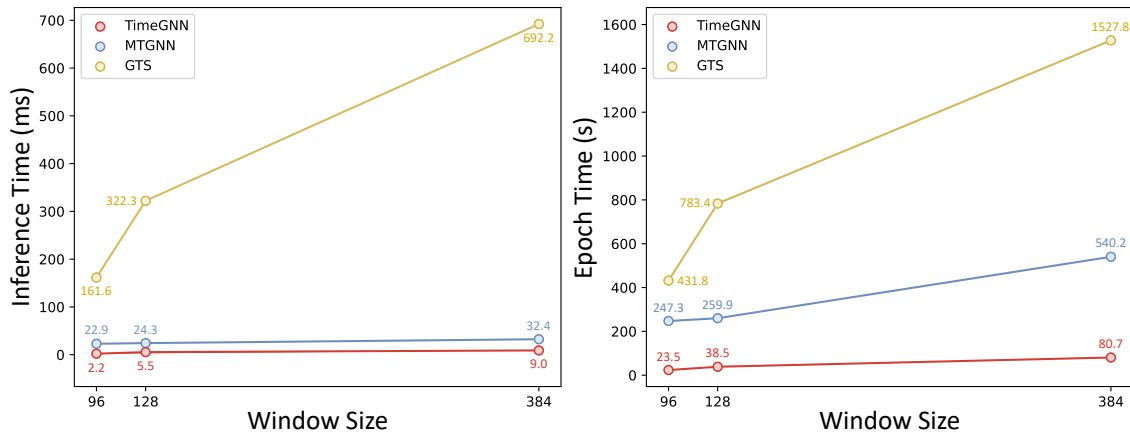


Figure 3: Computation cost of varying window sizes for graph-based models.

Table 1: Exchange-Rate Multivariate.

	Metric	LSTM	TCN	LSTN	GTS	MTGNN	TimeGNN
$h=1$	mse	0.328 ± 0.007	0.094 ± 0.118	0.004 ± 0.000	0.005 ± 0.001	0.006 ± 0.002	0.129 ± 0.012
	mae	0.475 ± 0.033	0.191 ± 0.163	0.033 ± 0.000	0.041 ± 0.004	0.048 ± 0.011	0.294 ± 0.029
	R^2	0.424 ± 0.013	0.834 ± 0.208	0.993 ± 0.000	0.992 ± 0.001	0.990 ± 0.003	0.773 ± 0.022
$h=3$	mse	0.611 ± 0.001	0.063 ± 0.035	0.013 ± 0.003	0.009 ± 0.000	0.012 ± 0.000	0.368 ± 0.059
	mae	0.631 ± 0.031	0.190 ± 0.041	0.078 ± 0.012	0.063 ± 0.000	0.078 ± 0.000	0.501 ± 0.045
	R^2	-0.078 ± 0.002	0.890 ± 0.061	0.978 ± 0.006	0.984 ± 0.000	0.979 ± 0.000	0.350 ± 0.104
$h=6$	mse	0.877 ± 0.105	0.189 ± 0.221	0.033 ± 0.005	0.014 ± 0.001	0.024 ± 0.001	0.354 ± 0.031
	mae	0.775 ± 0.032	0.290 ± 0.214	0.139 ± 0.008	0.081 ± 0.005	0.111 ± 0.000	0.453 ± 0.052
	R^2	-0.555 ± 0.185	0.665 ± 0.393	0.942 ± 0.008	0.975 ± 0.002	0.958 ± 0.002	0.371 ± 0.056
$h=9$	mse	0.823 ± 0.118	0.123 ± 0.030	0.030 ± 0.006	0.020 ± 0.001	0.035 ± 0.003	0.453 ± 0.149
	mae	0.743 ± 0.080	0.277 ± 0.037	0.124 ± 0.011	0.096 ± 0.001	0.140 ± 0.008	0.543 ± 0.084
	R^2	-0.465 ± 0.211	0.782 ± 0.053	0.946 ± 0.010	0.965 ± 0.001	0.938 ± 0.005	0.193 ± 0.265

4.4 Results

Scalability: We compare the inference and training times of TimeGNN with MTGNN and GTS, which also contain graph structure learning modules in Figure 2. GTS is the most computationally costly in both inference and training time due to the use of the entire training dataset for graph construction. In contrast, MTGNN learns static node features and is subsequently more efficient.

In inference time, there is relatively little difference between 8 and 12 variables for all models. However, when the number of variables increases to 321, there is a noticeable jump in inference time for MTGNN and GTS as their graph sizes increase. TimeGNN’s graph does not increase in size with the number of variables and consequently, the inference time remains constant across datasets. The training epoch times follow the observations in inference time. GTS remains the most costly followed by MTGNN and finally TimeGNN.

Since TimeGNN’s graph structure relies on the window size rather than the number of variables, the cost of increasing the window size on the Electricity-Load dataset is shown in Figure 3. As the window size increases, so does the cost of inference and training for all models. GTS rapidly becomes more costly as window size increases. As the graph learning module does not interact with the window size, the increase in cost can primarily be attributed to GTS’s encoder and decoder module for forecasting. Similarly, MTGNN’s graph learning module does not rely on the window size. MTGNN’s inference times do not increase as dramatically as GTS’s, showing the robustness of its forecasting modules. TimeGNN does not show significant growth in inference and training cost as the window size increases and remains the fastest of the GNN methods examined. This demonstrates that the graph learning module does not become overly cumbersome as window sizes vary.

Forecasting Quality: Table 1 summarizes the forecasting performance on the eight-variable Exchange-rate dataset for different horizons $h \in \{1, 3, 6, 9\}$. In general, GTS has the best forecasting performance on this dataset. Since the Exchange-rate dataset is quite small, the use of the training data during graph construction may give GTS an advantage over the other methods. TimeGNN however shows signs of overfitting during training and is unable to match the other two GNNs.

Table 2: Weather Multivariate.

	Metric	LSTM	TCN	LSTN	GTS	MTGNN	TimeGNN
h=1	mse	0.162 ± 0.001	0.176 ± 0.006	0.193 ± 0.001	0.209 ± 0.003	0.232 ± 0.008	0.178 ± 0.001
	mae	0.202 ± 0.003	0.220 ± 0.011	0.236 ± 0.002	0.213 ± 0.004	0.230 ± 0.002	0.185 ± 0.000
	R^2	0.824 ± 0.001	0.809 ± 0.006	0.790 ± 0.001	0.772 ± 0.003	0.748 ± 0.008	0.806 ± 0.001
h=3	mse	0.221 ± 0.000	0.232 ± 0.003	0.233 ± 0.001	0.320 ± 0.005	0.263 ± 0.003	0.234 ± 0.001
	mae	0.265 ± 0.000	0.275 ± 0.000	0.285 ± 0.000	0.320 ± 0.001	0.273 ± 0.000	0.249 ± 0.001
	R^2	0.759 ± 0.000	0.747 ± 0.004	0.746 ± 0.001	0.651 ± 0.005	0.713 ± 0.003	0.745 ± 0.001
h=6	mse	0.268 ± 0.004	0.274 ± 0.002	0.266 ± 0.001	0.374 ± 0.003	0.301 ± 0.003	0.287 ± 0.002
	mae	0.320 ± 0.004	0.323 ± 0.001	0.321 ± 0.000	0.388 ± 0.002	0.311 ± 0.002	0.297 ± 0.001
	R^2	0.708 ± 0.005	0.702 ± 0.003	0.711 ± 0.001	0.592 ± 0.003	0.672 ± 0.003	0.688 ± 0.002
h=9	mse	0.292 ± 0.007	0.307 ± 0.009	0.288 ± 0.000	0.399 ± 0.002	0.329 ± 0.001	0.316 ± 0.001
	mae	0.342 ± 0.003	0.350 ± 0.005	0.345 ± 0.003	0.420 ± 0.004	0.339 ± 0.004	0.331 ± 0.001
	R^2	0.682 ± 0.007	0.666 ± 0.010	0.686 ± 0.000	0.565 ± 0.003	0.642 ± 0.001	0.656 ± 0.001

Table 3: Electricity-Load Multivariate.

	Metric	LSTM	TCN	LSTN	GTS	MTGNN	TimeGNN
h=1	mse	0.226 ± 0.002	0.267 ± 0.001	0.064 ± 0.001	0.135 ± 0.002	0.046 ± 0.000	0.211 ± 0.003
	mae	0.323 ± 0.000	0.375 ± 0.002	0.167 ± 0.001	0.246 ± 0.001	0.131 ± 0.000	0.309 ± 0.001
	R^2	0.754 ± 0.002	0.709 ± 0.001	0.931 ± 0.001	0.853 ± 0.002	0.950 ± 0.000	0.770 ± 0.003
h=3	mse	0.255 ± 0.001	0.329 ± 0.015	0.065 ± 0.001	0.303 ± 0.019	0.079 ± 0.001	0.179 ± 0.003
	mae	0.339 ± 0.000	0.406 ± 0.013	0.163 ± 0.002	0.388 ± 0.019	0.171 ± 0.000	0.320 ± 0.002
	R^2	0.723 ± 0.001	0.642 ± 0.016	0.929 ± 0.001	0.670 ± 0.020	0.914 ± 0.001	0.829 ± 0.003
h=6	mse	0.253 ± 0.005	0.331 ± 0.010	0.125 ± 0.006	0.334 ± 0.000	0.097 ± 0.000	0.246 ± 0.004
	mae	0.340 ± 0.006	0.408 ± 0.009	0.238 ± 0.005	0.413 ± 0.000	0.189 ± 0.001	0.332 ± 0.004
	R^2	0.726 ± 0.005	0.640 ± 0.011	0.864 ± 0.006	0.637 ± 0.000	0.895 ± 0.001	0.732 ± 0.004
h=9	mse	0.271 ± 0.009	0.349 ± 0.022	0.144 ± 0.013	0.289 ± 0.021	0.108 ± 0.002	0.258 ± 0.010
	mae	0.351 ± 0.003	0.410 ± 0.019	0.251 ± 0.013	0.368 ± 0.020	0.198 ± 0.002	0.344 ± 0.007
	R^2	0.706 ± 0.010	0.621 ± 0.024	0.844 ± 0.014	0.686 ± 0.023	0.883 ± 0.002	0.719 ± 0.011

Table 2 contains the forecasting metrics for the twelve-variable Weather dataset. Here the purely recurrent methods perform the best in MSE and R^2 scores across all horizons. However, TimeGNN surpasses the recurrent methods on MAE scores, suggesting that TimeGNN is producing more significant outlier predictions than the recurrent methods. At the same time, TimeGNN remains competitive with the recurrent methods on the other metrics and is the best performing among the GNN methods.

Table 3 contains the forecasting metrics for the 321-variable Electricity-load dataset. MTGNN has in general the best forecasting performance, followed closely by LSTNet. TimeGNN falls behind the other GNN methods and underfits during training. This can be attributed to the large number of correlated variables in the dataset, which possibly makes the series correlations harder to be captured with time-domain graphs rather than correlation ones. However, it is important to highlight that TimeGNN still performs better than the LSTM and TCN benchmarks on this dataset.

5 Conclusion

We have presented a novel method of representing and dynamically generating graphs from raw time series. While conventional methods construct graphs based on the variables, we instead construct graphs such that each time step is a node. We use this method in TimeGNN, a model consisting of a graph construction module and a simple GNN-based forecasting module, and examine its performance against state-of-the-art neural networks, including some that perform jointly graph learning and forecasting. While TimeGNN’s relative performance differs between datasets, this representation is clearly able to capture and learn the underlying properties of time series. Additionally, it is far faster and more scalable than existing graph methods as both the number of variables and the window size increase. However, there are several avenues for further improvement. The forecasting module, purposefully kept simple in order to examine the effects of the learnable temporal representations, could be extended to a more complex architecture. The graph learning module could also be modified to include edge weights learned on separately extracted features.

Acknowledgments

The computations were enabled by resources provided by the National Academic Infrastructure for Supercomputing in Sweden (NAISS) at ALVIS partially funded by the Swedish Research Council through grant agreement no. 2022-06725.

References

- [1] Xiao Ding, Yue Zhang, Ting Liu, and Junwen Duan. Deep learning for event-driven stock prediction. In *Twenty-fourth international joint conference on artificial intelligence*, 2015.
- [2] Yaguang Li, Rose Yu, Cyrus Shahabi, and Yan Liu. Diffusion convolutional recurrent neural network: Data-driven traffic forecasting. *arXiv preprint arXiv:1707.01926*, 2017.
- [3] Sucheta Chauhan and Lovekesh Vig. Anomaly detection in ecg time signals via deep long short-term memory networks. In *2015 IEEE international conference on data science and advanced analytics (DSAA)*, pages 1–7. IEEE, 2015.
- [4] George EP Box, Gwilym M Jenkins, Gregory C Reinsel, and Greta M Ljung. *Time series analysis: forecasting and control*. John Wiley & Sons, 2015.
- [5] Bryan Lim and Stefan Zohren. Time-series forecasting with deep learning: a survey. *Philosophical Transactions of the Royal Society A*, 379(2194):20200209, 2021.
- [6] David E Rumelhart, Geoffrey E Hinton, and Ronald J Williams. Learning representations by back-propagating errors. *nature*, 323(6088):533–536, 1986.
- [7] Yann LeCun, Léon Bottou, Yoshua Bengio, and Patrick Haffner. Gradient-based learning applied to document recognition. *Proceedings of the IEEE*, 86(11):2278–2324, 1998.
- [8] Yulia Rubanova, Ricky TQ Chen, and David K Duvenaud. Latent ordinary differential equations for irregularly-sampled time series. *Advances in neural information processing systems*, 32, 2019.
- [9] David W Romero, Anna Kuzina, Erik J Bekkers, Jakub M Tomczak, and Mark Hoogendoorn. Ckconv: Continuous kernel convolution for sequential data. *arXiv preprint arXiv:2102.02611*, 2021.
- [10] Vincent Le Guen and Nicolas Thome. Deep time series forecasting with shape and temporal criteria. *IEEE Transactions on Pattern Analysis and Machine Intelligence*, 45(1):342–355, 2022.
- [11] Chrysoula Kosma, Giannis Nikolentzos, Nancy Xu, and Michalis Vazirgiannis. Time series forecasting models copy the past: How to mitigate. In *Artificial Neural Networks and Machine Learning—ICANN 2022: 31st International Conference on Artificial Neural Networks, Bristol, UK, September 6–9, 2022, Proceedings, Part I*, pages 366–378. Springer, 2022.
- [12] François Rousseau and Michalis Vazirgiannis. Graph-of-word and tw-idf: new approach to ad hoc ir. In *Proceedings of the 22nd ACM international conference on Information & Knowledge Management*, pages 59–68, 2013.
- [13] Zonghan Wu, Shirui Pan, Guodong Long, Jing Jiang, Xiaojun Chang, and Chengqi Zhang. Connecting the dots: Multivariate time series forecasting with graph neural networks. In *Proceedings of the 26th ACM SIGKDD international conference on knowledge discovery & data mining*, pages 753–763, 2020.
- [14] Defu Cao, Yujing Wang, Juanyong Duan, Ce Zhang, Xia Zhu, Congrui Huang, Yunhai Tong, Bixiong Xu, Jing Bai, Jie Tong, et al. Spectral temporal graph neural network for multivariate time-series forecasting. *Advances in neural information processing systems*, 33:17766–17778, 2020.
- [15] Chao Shang, Jie Chen, and Jinbo Bi. Discrete graph structure learning for forecasting multiple time series. *arXiv preprint arXiv:2101.06861*, 2021.
- [16] Lucas Lacasa, Bartolo Luque, Fernando Ballesteros, Jordi Luque, and Juan Carlos Nuno. From time series to complex networks: The visibility graph. *Proceedings of the National Academy of Sciences*, 105(13):4972–4975, 2008.
- [17] Reik V Donner, Yong Zou, Jonathan F Donges, Norbert Marwan, and Jürgen Kurths. Recurrence networks—a novel paradigm for nonlinear time series analysis. *New Journal of Physics*, 12(3):033025, 2010.
- [18] James Douglas Hamilton. *Time series analysis*. Princeton university press, 2020.
- [19] Sepp Hochreiter and Jürgen Schmidhuber. Long short-term memory. *Neural computation*, 9(8):1735–1780, 1997.
- [20] Kyunghyun Cho, Bart Van Merriënboer, Caglar Gulcehre, Dzmitry Bahdanau, Fethi Bougares, Holger Schwenk, and Yoshua Bengio. Learning phrase representations using rnn encoder-decoder for statistical machine translation. *arXiv preprint arXiv:1406.1078*, 2014.
- [21] Shaojie Bai, J Zico Kolter, and Vladlen Koltun. An empirical evaluation of generic convolutional and recurrent networks for sequence modeling. *arXiv:1803.01271*, 2018.

- [22] Guokun Lai, Wei-Cheng Chang, Yiming Yang, and Hanxiao Liu. Modeling long-and short-term temporal patterns with deep neural networks. In *The 41st international ACM SIGIR conference on research & development in information retrieval*, pages 95–104, 2018.
- [23] Boris N Oreshkin, Dmitri Carпов, Nicolas Chapados, and Yoshua Bengio. N-beats: Neural basis expansion analysis for interpretable time series forecasting. *arXiv preprint arXiv:1905.10437*, 2019.
- [24] Ashish Vaswani, Noam Shazeer, Niki Parmar, Jakob Uszkoreit, Llion Jones, Aidan N Gomez, Łukasz Kaiser, and Illia Polosukhin. Attention is all you need. *Advances in neural information processing systems*, 30, 2017.
- [25] Haoyi Zhou, Shanghang Zhang, Jieqi Peng, Shuai Zhang, Jianxin Li, Hui Xiong, and Wancai Zhang. Informer: Beyond efficient transformer for long sequence time-series forecasting. In *Proceedings of the AAAI conference on artificial intelligence*, volume 35, pages 11106–11115, 2021.
- [26] Haixu Wu, Jiehui Xu, Jianmin Wang, and Mingsheng Long. Autoformer: Decomposition transformers with auto-correlation for long-term series forecasting. *Advances in Neural Information Processing Systems*, 34:22419–22430, 2021.
- [27] Steven Kearnes, Kevin McCloskey, Marc Berndl, Vijay Pande, and Patrick Riley. Molecular graph convolutions: moving beyond fingerprints. *Journal of computer-aided molecular design*, 30:595–608, 2016.
- [28] Vladimir Gligorijević, P Douglas Renfrew, Tomasz Kosciółek, Julia Koehler Leman, Daniel Berenberg, Tommi Vatanen, Chris Chandler, Bryn C Taylor, Ian M Fisk, Hera Vlamakis, et al. Structure-based protein function prediction using graph convolutional networks. *Nature communications*, 12(1):3168, 2021.
- [29] Justin Gilmer, Samuel S Schoenholz, Patrick F Riley, Oriol Vinyals, and George E Dahl. Neural message passing for quantum chemistry. In *International conference on machine learning*, pages 1263–1272. PMLR, 2017.
- [30] Bing Yu, Haoteng Yin, and Zhanxing Zhu. Spatio-temporal graph convolutional networks: A deep learning framework for traffic forecasting. *arXiv preprint arXiv:1709.04875*, 2017.
- [31] Youngjoo Seo, Michaël Defferrard, Pierre Vandergheynst, and Xavier Bresson. Structured sequence modeling with graph convolutional recurrent networks. In *Neural Information Processing: 25th International Conference, ICONIP 2018, Siem Reap, Cambodia, December 13-16, 2018, Proceedings, Part I 25*, pages 362–373. Springer, 2018.
- [32] Ling Zhao, Yujiao Song, Chao Zhang, Yu Liu, Pu Wang, Tao Lin, Min Deng, and Haifeng Li. T-gcn: A temporal graph convolutional network for traffic prediction. *IEEE transactions on intelligent transportation systems*, 21(9):3848–3858, 2019.
- [33] Thomas Kipf, Ethan Fetaya, Kuan-Chieh Wang, Max Welling, and Richard Zemel. Neural relational inference for interacting systems. In *International conference on machine learning*, pages 2688–2697. PMLR, 2018.
- [34] Eric Jang, Shixiang Gu, and Ben Poole. Categorical reparameterization with gumbel-softmax. *arXiv preprint arXiv:1611.01144*, 2016.
- [35] Min Lin, Qiang Chen, and Shuicheng Yan. Network in network. *arXiv preprint arXiv:1312.4400*, 2013.
- [36] Will Hamilton, Zhitao Ying, and Jure Leskovec. Inductive representation learning on large graphs. *Advances in neural information processing systems*, 30, 2017.